



Science

## **COMPUTING THE EFFICIENCY OF IMAGE SEGMENTATION TECHNIQUES IN FMRI ANALYSIS**

**Arthi. C<sup>\*1</sup>, Dr.Savithri<sup>2</sup>**

<sup>\*1</sup>Post graduate student of M.Sc. CST, Women's Christian College, Chennai-06, India

<sup>2</sup>Assistant Professor, Women's Christian College, Chennai-06,

India DOI: <https://doi.org/10.29121/granthaalayah.v5.i3.2017.1772>



### **Abstract**

Functional magnetic resonance imaging has become a very popular tool in neurological and medical analysis over the years. According to collated data, in the year 1993, as few as 20 papers were presented on the topic of fmri analysis; However, a decade later, as many as 1800 research papers talk about fmri analysis – an exponential increase. An analysis of the activated regions within the brain can be used to detect the its reactions to various stimuli with greater confidence compared to other methods but the success of accurately identifying brain stimuli however lies in the efficiency of the image processing algorithms applied to extract information from the fMRI scans. This paper analyzes the effectiveness of commonly used image processing algorithms in fMRI studies by statistically analyzing their effectiveness in extracting ROI's in various images (sample size = 17) and tries to project the efficiency of these systems in fMRI scanning.

**Keywords:** FMRI, Image Processing Algorithms; K-Means; HSV Segmentation; OTSU Segmentation; Delta-E Segmentation.

**Cite This Article:** Arthi. C, and Dr.Savithri. (2017). "COMPUTING THE EFFICIENCY OF IMAGE SEGMENTATION TECHNIQUES IN FMRI ANALYSIS." *International Journal of Research - Granthaalayah*, 5(3), 223-237. 10.29121/granthaalayah.v5.i3.2017.1772.

### **1. Introduction**

In day to day life, various factors determine how we react to situations, how we perceive things and how a variety of stimuli consciously or subconsciously impact the course of various events. We go through several emotions and perform various actions on a daily basis. There are thought processes, quick decision making, cognitive dissonance, learning, lying etc that rely heavily on the brain's ability to process external information. Racine et al(2005) point out that fmri analysis has brought about hope that this non-invasive procedure could instigate a deeper understanding of basic human phenomena such as emotion and cognition. Knutsen et al, (2004) aptly suggest that mental states within the human brain are fickle and the need of the hour therefore lies in

effectively capturing their traces before they fade away. This, according to them, requires temporal and spatial precision. They further point out that although numerous techniques have been devised to read brain signals, they are hampered by various tradeoffs resulting in lower temporal or spatial resolutions.

Patterns exist in daily life - behaviour and thought processes are often impinged upon reactions to stimuli and circumstances. For instance, Vrij(2000) points out that lying is banal and commonplace and that people tend to lie every day in some situation or the other. Saxe(2016) provides a different perspective to the same context. He points out that although people are socialized to believe that it is better to tell the truth, situations and circumstances often encourage and reward deceptive behavior. This common notion of lying has different connotations in different contexts. Depaulo(2004) suggests that humans tend to exhibit a bias naturally in everyday life. She posits that even the simplest of questions have several connotations and that responses are often based on underlying goals that people currently are trying to pursue. From simple tasks to the most complex behaviour, everything is a reaction to external stimuli. In order to therefore understand human behaviour, one needs to peer into the brain and understand the underlying *psychosomatic* characteristics that elicit these behaviours. It is therefore important to detect and understand various patterns that originate in the brain and correlate them with external activities.

Non invasive scientific analysis of the human mind was restricted to one of three things – (a) observing underlying behaviour(body language) (b) Analysis of speech and sensory stimuli (c) by employing techniques to measure physiological changes to situations. However these methods did not directly give us vital clues into the inner workings of the brain and how each of these processes was interlinked. Kesavadas et al (2007), suggest that traditionally, mapping of relevant areas in the human brain is achieved through invasive methods such as *intra operative cortical stimulation* in a patient using the subdural grid and calculating sensory potentials using intraoperative recording. These methods although accurate, are extremely invasive and potentially dangerous.

According to them, fMRI scans achieve similar accuracy and can help obtain the necessary information non-invasively and most importantly without any need for surgical intervention. (Boynton et al., 1996; Buckner et al.,1996) note that fmri scans have the capacity to rapidly measure hemodynamic responses to fast changing external conditions and are highly sensitive to changes in hemoglobin levels in the brain. These transient traces can therefore be used to detect numerous things in clinical and medical analysis – it has been proven that fMRI analyses can help predict potential deficits in cognitive functions such as speech, visual, language and motor functions. Several neurological studies have shown that there are significant differences in brain stimulus related to recognition of events (Cabeza et al, 2007). (Suzuki et al, 2008) in their studies were able to map numerous executive functions in the brain; In particular, they were able to establish that the left prefrontal cortex and the right anterior hippocampus were activated during cognition and during deceit. The role of technology in these studies is implicit and is well established. Advances in image processing and magnetic imaging techniques have paved way for accurate identification of various areas of the brain. Correlating external stimuli with elevated brain function is now possible because of advances in image processing algorithms. Image analysis therefore is an important precursor to data analysis in such studies.

(Smith et al, 2004) imply that the primary challenge in the analysis of fMRI scans is to identify *voxels* which show varying signal changes according to different brain states. FMRI scans exhibit poor signal to noise ratio with signal strengths often coinciding with equivalent noise levels in the output scanned image. The reliability of cognitive studies therefore depends on the efficiency and the accuracy of the underlying image processing algorithms. (Despotovic et al, 2015) lay emphasis on the importance of image segmentation in clinical studies. They highlight that brain MRI segmentation is vital to the outcome of practical analysis since it accurately *slices* different anatomical regions of the brain based on a varied set of input parameters. Evidence suggests that such image processing algorithms are practically used in scientific and clinical analysis. For example, surgical planning of procedures on tumors and lesions in the brain are guided by precision image analysis. It is therefore vital to measure the efficiency and the accuracy of *image segmentation algorithms* that are applied during fMRI studies.

This paper will explore fundamental image processing algorithms and try to ascertain empirically their efficiency, accuracy in delineating *voxels* through a mediated analysis of its software performance. Segmentation techniques were selected based on the *applied frequency* of their use in practical studies. The MATLAB software system was used to devise programs based on the algorithms therein using various image processing methods such as *morphological image opening and closing* as the basis for segmentation. The image processing toolkit within MATLAB was primarily used to write the programs. A standard image size and a sample set of 17 images was considered for this study. Each scan image in the set was subjected to these segmentation algorithms and the output visually analyzed. Numerous data points were accrued and analyzed based on standard baseline control values for validity and deviations. F1 scores were also calculated and the results finally tabled.

## 2. Literature Review

### 2.1.Historical Background

The human brain is an enigma unto itself. The most important organ in the human body is the least understood component of the human psyche. The brain is the seat of knowledge, identity, behavior and emotion. It drives all aspects of intellect, emotion, physiology and psychology in humans and yet, studies have not been able to fully understand the inner workings of the human brain. Numerous studies have tackled various problems – psychological, neurobiological, functional, brain mapping studies, behavior analysis; medical science has abundant reasons to unearth potential cures to myriad problems through brain studies. While the area of study is large and voluminous, humans have been curious about the brain and its inner workings from time immemorial.

The earliest archeological evidence of humans having a perception about the brain comes from cave paintings and remains found in France, dating back to the *Neolithic* period. Cave paintings have detailed the practice of *trephination* or *trepanning* - one of the earliest *applied surgical methods* to alleviate pressure and pain. It was believed that burr holing or *trephination* would cure epileptic seizures, migraines and mental disorders which in modern medicine has become a valid technique to cure sub-cranial and epidural hematomas (*craniotomy*).

The knowledge that the brain was the center of the human nervous system was also asserted by Hippocrates in first century B.C. Hippocrates speculated that the human brain had a mental duality and posited that the two halves of the brain were capable of independent functioning.

Although there was a rudimentary understanding about the human brain, it wasn't until the early 17<sup>th</sup> century that theories about the human brain were formulated. In the early 17<sup>th</sup> century, Thomas Willis wrote the *Cerebri anatome*, wherein he postulated that the cerebral cortex was the seat of cognition. He studied the meninges and claimed that the pain responses originated from the base of the brain. The anastomosis within the brain was rigorously studied by him – a first in modern medicine.

Although significant strides were made in the past, most of them involved dissecting the human brain and trying to ascertain the inner workings of the brain. It wasn't until the late 19<sup>th</sup> century that live stimulus brain mapping case studies were carried out. The first breakthrough in mapping brain regions happened when Penfield induced cortical stimulation in patients undergoing neurosurgery. The technique was refined to map the motor and somatic sensory regions in the cortex of the brain.

The early 70's saw the advent of *computed tomography* wherein short x-ray pulses were applied to render slices of each organ where these rays passed through. Fifteen years ago, Functional magnetic resonance imaging (fMRI), a non-invasive procedure was developed to map human brain regions and functions. Functional magnetic resonance imaging (fMRI) was launched as a method to analyze the changes in local blood flow and hemodynamic of the brain that directly correspond to the elevated neuronal activities accompanied by metabolic impulses. It paved the way to map the human brain's anatomical structures and helped narrow down specific functions within the brain. With advances in high technology, high resolutions were achieved. These images captured by highly sensitive imaging equipment allowed doctors to purview neural activity by means of a blood oxygen level dependent signal. The oxygen concentration in brain can be used as a tool to map various *voxels* in the brain responsible for several cognitive functions. Over time, fMRI has become commonplace because of its non-invasive nature. It is easy to operate, is highly reliable, provides high resolution images that can be easily reproduced and does not involve the use of any external contrast inducing agents. Most importantly, fMRI images can be produced without any major change to existing scanners. Almost all existing MR scanners can be used to procure fMRI data. fMRI yields superior temporal and spatial resolution relative to other functional imaging techniques. fMRI(s) have become a prominent tool in modern medical diagnostics and is increasingly being prescribed as a way to diagnose problems and manage patients. Numerous medical practitioners are using fMRI techniques in areas such as clinical neuropsychology, neurology, surgery, psychiatry and rehabilitation to improve patient care and elevate the standard of medicine, thereby improving the patient's quality of life. The best developed clinical application has involved the use of fMRI in the pre-surgical mapping of patients with brain tumors and epilepsy.

## 2.2. Image Processing

According to (Despotović et al, 2015), image segmentation is one of the most critical tasks in medical image analysis and is often the first and the most critical step in many clinical applications. They suggest that in brain MRI analysis, image segmentation is commonly used for

measuring and visualizing the brain's anatomical structures, for analyzing brain changes, and for identifying pathology. It has become a necessary pre-requisite in surgical planning and has been used for advanced image guided procedures.

Nourouzi et al (2014) posit that image segmentation is the most important aspect in medical image processing since it involves the extraction of Regions of interest (ROI) which is the most important step to analyzing medical imagery. It is important to extract the underlying region without compromising quality. Disadvantages like noise, intensity in homogeneities, low contrast between certain tissues, and partial volume effects can hamper image segmentation and appropriate algorithms must therefore be selected to distinctly extract the intended regions of interest. Interpretation of results is heavily reliant on the success of various algorithms employed to extract practical data.

(Wee et al, 2006), describe three broad fMRI segmentation algorithm categories that when used in different contexts yield different segmentation accuracy and result in the segmentation of the fmr images of the brain. They classify the algorithms into: region-based, classification based and contour-based segmentation paradigms.

For the purpose of this study, classification and region based techniques were selected based on the analysis of their applied frequency in previous fMRI studies. Table 1 shows the list of algorithms chosen for this study.

Technique	Algorithm Chosen
Clustering	K-Means clustering
Color Based Separation	Image Segmentation using HSV color spaces Delta E Segmentation
Thresholding	OTSU thresholding algorithm

### 3. Materials and Methods

#### 3.1. Proposed System

##### Image segmentation using HSV Color Spaces:

An image can be thought of as a composite collection of various objects and regions cohesively grouped according to colour. Image segmentation is a set of techniques that when used appropriately, accurately extracts information from it. (Kumar et al, 2016) suggest that the application of image segmentation algorithms depends on two important properties that every image has – a) discontinuity b) similarity.

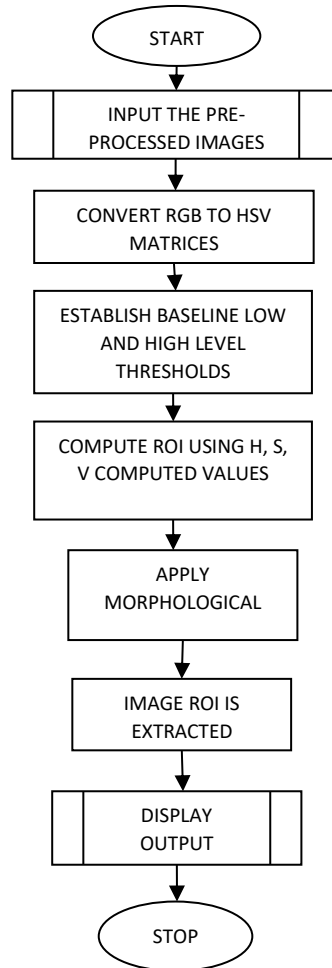
Algorithms that approach segmentation of images on the basis of discontinuity tend to analyze regions of isolation within each image and partition regions based on these incongruencies. Color segmentation on the other hand tries to classify the images based on pixel patterns that are similar in nature. (Bora et al, 2015) define color segmentation as a process of extricating from the image connected regions satisfying conditions of homogeneity.

Color spaces: A color space is actually a specific organization of colors that allows us to denote colors as a series of contiguous digital representations. In the HSV colour space, each color is represented by unique hue, saturation and value components with Hue representing the color, saturation representing the dominance of the color and value representing the brightness of the color.

The HSV color space can be diagrammatically represented as a cone. For a given point (h, s, v) in the cone, h and s are the angular and radial coordinates of the point on a disk of radius v. This can be used as the basis to segment images based on regions of color and continuity.

The following steps capture the programmatic implementation of the algorithm in this study.

- Step 1: Read fMRI image.
- Step 2: convert image to individual HSV matrices.
- Step 3: Establish baseline low and high thresholds for hue, saturation and value.
- Step 4: Compute Hue, Saturation and value components for intended Region of interest (activated regions of the temporal/pre-frontal cortex)
- Step 5: Total number of colors existing in an original image is calculated by morphological dilation and compositing.
- Step 6: Image is partitioned and the intended region is reconverted back to RGB.



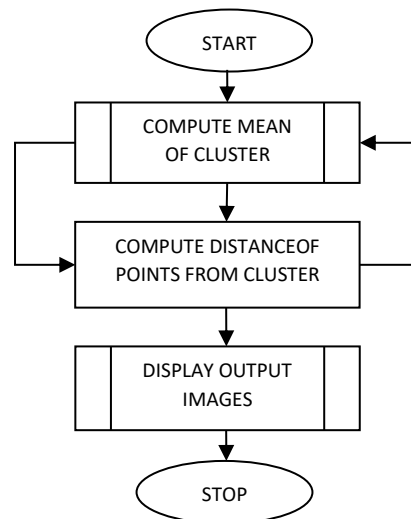
## K-means clustering

The k-means method aims to minimize the sum of squared distances between all points and the cluster centre. Given a set of data points  $d$  in space  $R$ , the algorithm tries to find the set of points  $k$  in  $R(d)$  that have minimal *squared error distortion*.

The k-means algorithm therefore tries to find an optimally distinct set of data points that have minimal clustering error. The algorithm is iterative and starts with a cluster that initially is picked out randomly and then proceeds to minimize the clustering error by iteratively grouping similarly matching regions within the image.

The algorithm is implemented as follows:

- 1) Compute the mean of each cluster.
- 2) Compute the distance of each point from each cluster by computing its distance from the corresponding cluster mean.
- 3) Iterate over the above steps till the sum of squared is grouped within cluster means.



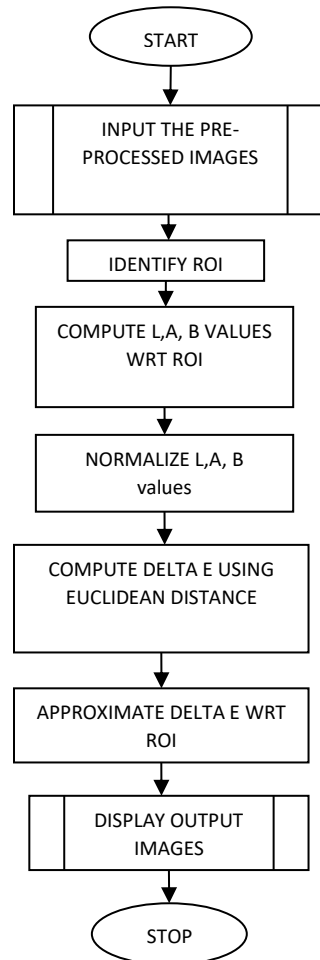
## Delta-E segmentation

The difference or distance between two colors is a metric of interest in color science. It allows quantified examination of a notion that formerly could only be described with adjectives. Quantification of these properties is of great importance to those whose work is color critical. Common definitions make use of the Euclidean distance in a device independent color space. The distance metric that is commonly used to denote the intrinsic difference between two colors in the rgb color space is known as  $\Delta E$ . DeltaE represents the 'distance' between two colors and is denoted by a single number. A value of 1.0 in the Delta E scale represents the smallest color difference that the human eye can perceive. The proposed system tries to distinguish colors and separate them in the fmri image using possible deltaE differences between the regions analyzed.

The implementation is as follows:

- Step 1: Read RGB fMRI image.
- Step 2: Identify ROI from fMRI using boundary analysis.

- Step 3: Compute L, A, B vectors for image vis a vis ROI.
- Step 4: Normalize L, A, B values.
- Step 5: Compute Delta E using Euclidean distance measure.
- Step 6: Approximate delta E with respect to ROI.
- Step 7: Highlight ROI in image.



## Otsu segmentation

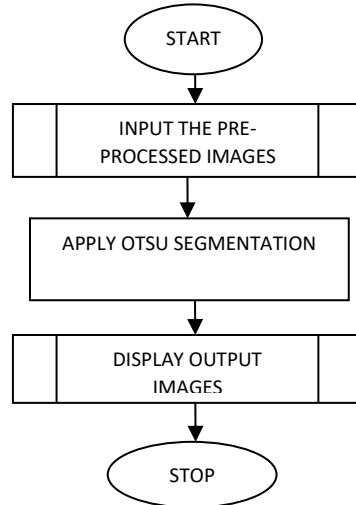
Otsu's method is used to perform clustering-based image thresholding, or, the reduction of a gray level image to a binary image. The algorithm assumes that the image contains two classes of pixels following bi-modal histogram (foreground pixels and background pixels), it then calculates the optimum threshold separating the two classes so that their combined spread (intra-class variance) is minimal, or equivalently (because the sum of pair-wise squared distances is constant), so that their inter-class variance is maximal.

The following steps were undertaken to implement OTSU's method programmatically:

- Step 1: read an RGB fMRI image.
- Step 2: Apply thresholding – morphological erosion and extraction of foreground objects using structuring element.



- Step 3: Adjust contrast variance post RGB to Grayscale conversion.
- Step 4: Morphological opening to find ROI.
- Step 5: Find all connected components based on contrast thresholds and label them.
- Step 6: Convert grayscale to RGB.



#### 4. Results and Discussions

The best way to analyze image information is by using one's visual acuity. The images below show the marked differences between the original image and the ROI's extracted by the application of various image segmentation algorithms. As can be seen from the images below, the ROI is extracted almost without any loss of information in the HSV color sampling algorithm. The K Means algorithm shows slight deviation from the expected output whilst the modified Delta E algorithm computes the ROI incorrectly leaving out some portions of the expected regions during its extraction. The OTSU segmentation algorithm overcompensates during computation and extracts extra portions from the image based on thresholds applied.

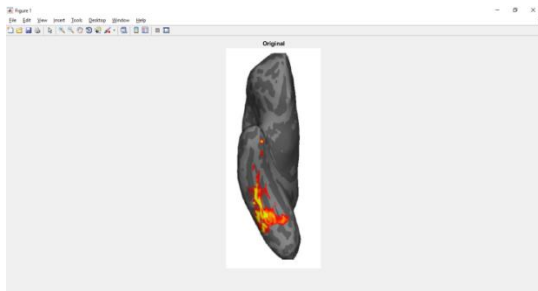


Figure 1: Original Image Baseline

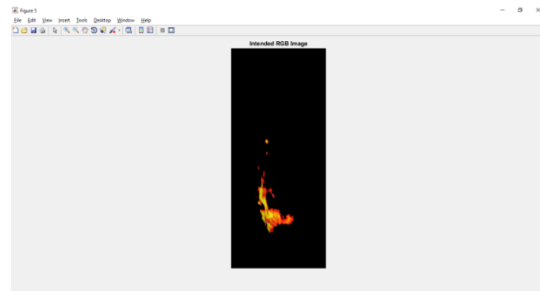


Figure 2: HSV: very minimal variations

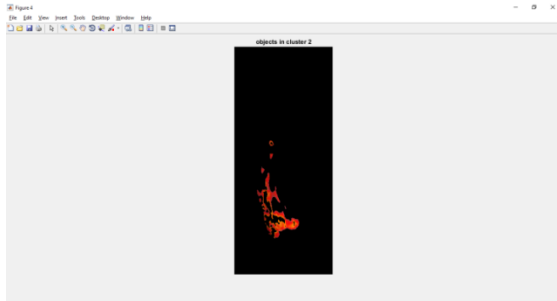


Figure 3: KMeans: minor deviations

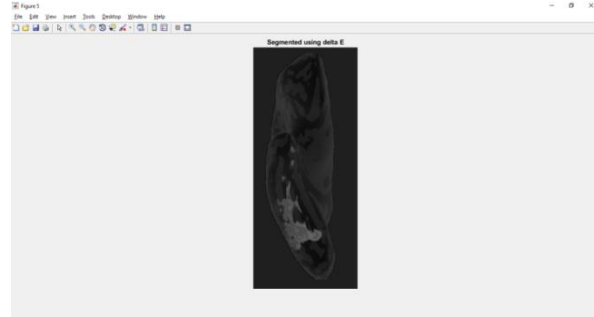


Figure 4: Delta E: Incomplete ROI Extraction

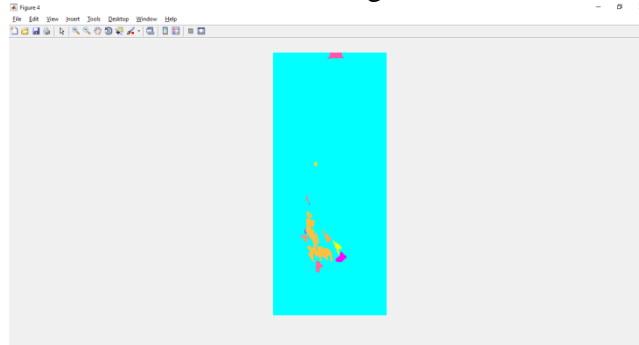


Figure 5: OTSU: over compensated ROI Extraction

The findings presented above were analyzed programmatically by calculating the ROI area matrices of various algorithms along with baseline.

### ROI Matrices

```
baseline = [ 220 118 18; 255 138 14; 243 85 0; 241 75 0; 167 90 80;
128 50 1; 125 4 9; 245 137 36; 226 154 34; 225 52 45; 195 175 186;
245 22 14; 212 80 91; 151 127 143; 248 40 12; 213 41 37; 185 24 6;
64 0 8; 255 18 5; 117 53 54; 239 254 3; 253 123 1; 253 210 10;
242 253 13; 247 110 6; 254 225 27; 255 24 7; 209 44 16; 253 242 10;
212 30 19; 20 0 0; 240 255 6; 162 28 29; 250 247 20; 255 242 25;
255 239 15; 245 175 2; 11 0 0; 222 106 31; 149 102 24; 19 0 0;
205 78 9; 0 0 2; 238 255 18; 252 127 0; 255 209 30; 247 246 16;
94 41 25; 250 251 10; 243 255 7; 249 248 10; 245 255 19; 239 247 6;
239 254 1; 252 147 22; 186 43 3; 249 216 0; 6 0 0; 62 1 0; 255
170 1; 243 255 3; 250 248 13; 251 250 12; 133 107 108; 153 108 111;
206 74 35; 216 27 25; 255 41 10; 254 21 16; 155 88 62; 178 88 97;
255 231 25; 255 164 18; 221 99 0; 250 177 20; 55 83 86; 134 60 33;
253 209 14; 255 68 10; 254 197 6; 100 26 13; 254 102 16; 255 132
11; 166 94 70; 196 156 154; 194 96 93; 232 78 8; 255 179 17; 252 57
9; 253 63 11; 255 248 22; 143 60 46; 251 196 7; 84 110 111; 172 97
32; 199 35 8; 197 22 0; 62 90 76; 154 26 23; 250 253 16; 240 245
3; 255 124 9; 255 142 3];
```

kMeans = [255 196 34; 242 251 4; 244 252 11; 0 0 0; 246 250 13;  
246 196 1; 236 255 11; 248 249 8; 255 207 34; 242 251 2; 172 143  
41; 241 255 10; 194 167 28; 242 250 7; 245 247 0; 243 255 7; 250 246  
15; 251 218 17; 255 244 14; 255 236 12; 247 153 5; 0 0 0; 0 0  
0; 0 0 0; 244 252 11; 244 251 15; 250 252 19; 0 0 0; 255 164 17;  
0 0 0; 255 179 37; 255 215 11; 244 252 21; 0 0 0; 0 0 0; 0  
0 0; 0 0 0; 244 235 10; 0 0 0; 0 0 0; 0 0 0; 250 224 13;  
247 252 27; 0 0 0; 245 255 14; 248 251 14; 240 252 6];

hsv = [ 255 189 31; 240 215 1; 0 0 0; 246 250 13; 243 253 16; 0 0  
0; 19 23 8; 241 148 0; 245 160 17; 190 42 2; 0 0 0; 194 61 42;  
243 253 9; 88 55 14; 254 242 16; 245 247 16; 252 250 15; 139 76 0;  
248 183 3; 255 143 17; 248 254 10; 0 0 0; 0 0 0; 0 0 0; 250  
64 13; 223 30 25; 0 0 0; 0 0 0; 248 20 7; 0 0 0; 240 62  
36; 127 40 23; 249 235 16; 255 189 17; 231 114 0; 255 39 5; 248 146  
10; 0 0 0; 109 36 21; 248 52 4; 255 112 8; 253 32 13; 246 114  
3; 223 33 43; 255 61 19; 255 220 21; 223 40 8; 214 27 18; 160 47  
41; 253 163 7; 255 250 18; 191 71 47; 214 60 36; 0 0 0; 48 9 2;  
255 88 20; 242 43 1; 0 0 0; 248 30 0; 244 255 13; 147 56 11;  
172 82 74; 248 153 7; 255 243 30; 249 103 4; 247 251 6; 243 173 26;  
255 147 3; 252 65 0; 158 20 10; 253 15 12; 254 225 27; 236 250 4;  
255 53 18; 0 0 0; 252 18 9; 211 38 31; 226 58 19; 217 83 82;  
219 55 18; 0 0 0; 0 0 0; 250 111 6; 255 238 38; 0 0 0; 0  
0 0; 211 81 32; 116 37 0; 253 146 4; 255 218 37; 247 116 25; 255  
82 6; 213 67 16; 0 0 0; 0 0 0; 0 0 0; 0 0 0; 0 0 0; 0  
0 0; 243 103 18; 247 82 2; 255 245 11; 245 254 7; 247 251 14; 240  
250 5; 243 227 7; 0 0 0; 251 251 15; 6 0 0; 252 246 0; 246 47  
5; 244 249 7; 241 255 5; 0 0 0; 255 244 18; 252 47 18];

deltaE = [0 31 0; 31 0 0; 255 255 255; 255 255 255; 255 255 255; 255  
255 255; 255 255 255; 255 255 255; 255 255 255; 255 255 255; 255 255 0;  
255 150 0; 186 0 124; 255 255 255; 255 255 255; 62 31 0; 0 90 0;  
0 0 0; 255 255 255; 255 255 255; 255 255 0; 255 255 255; 108 255 255;  
255 255 255; 124 0 0; 255 255 255; 255 255 255; 0 0 0; 31 0 0;  
255 255 255; 255 255 255; 255 255 255; 255 255 0; 255 255 198; 255 255  
105; 255 255 255; 255 255 255; 255 255 255; 255 255 255; 255 255 255;  
255 255 255; 255 255 255; 255 255 255; 255 0 0; 0 90 30; 255 255  
255; 255 255 0; 62 31 0; 255 255 0; 255 232 58];

otsu = [255 237 18; 255 237 18; 255 237 18; 255 237 18; 0 255 255; 255  
237 18; 255 237 18; 255 237 18; 255 237 18; 255 237 18; 255 237 18;  
255 237 18; 255 146 109; 255 146 109; 255 146 109; 255 146 109; 255 146  
109; 0 255 255; 0 255 255; 255 146 109; 255 146 109; 255 146 109; 255  
146 109; 255 146 109; 255 146 109; 0 255 255; 255 146 109; 255 146 109;  
255 146 109; 255 146 109; 255 146 109; 0 255 255; 0 255 255; 255 146  
109; 255 146 109; 255 146 109; 0 255 255; 0 255 255; 0 255 255; 255

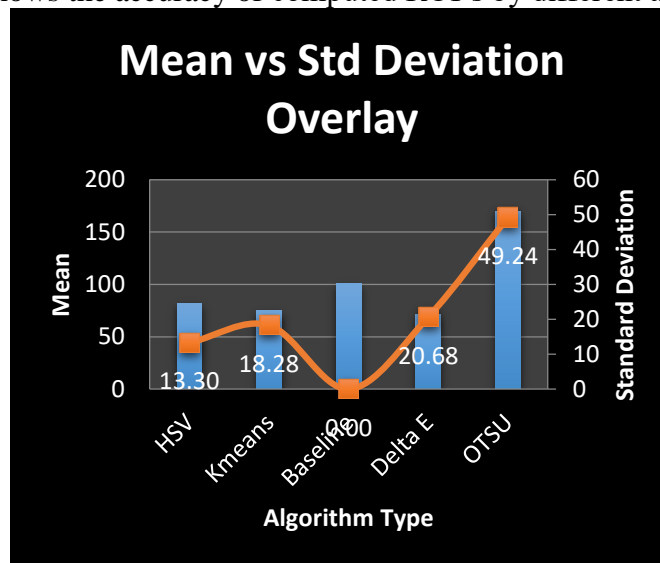
146 109; 255 146 109; 0 255 255; 255 146 109; 255 219 36; 255 219 36;  
 0 255 255; 255 219 36; 255 237 18; 255 237 18; 255 237 18; 255 237  
 18; 255 237 18; 255 237 18; 0 255 255; 255 237 18; 0 255 255; 255 73  
 182; 255 73 182; 0 255 255; 255 73 182; 0 255 255; 255 73 182; 0  
 255 255; 0 255 255; 0 255 255; 0 255 255; 255 0 255; 255 0 255; 255  
 0 255; 0 255 255; 255 182 73; 255 182 73; 255 182 73; 255 182 73; 255  
 182 73; 255 182 73; 255 182 73; 255 182 73; 255 182 73; 0 255 255; 0  
 255 255; 255 36 219; 0 255 255; 255 36 219; 255 36 219; 255 36 219];

The mean and standard deviation of the ROI pixel area matrix values were computed programmatically and the findings tabulated below:

Algorithm	Mean	Std Deviation
Baseline	100.3642	0
HSV	81.5484	13.30477977
KMeans	74.5137	18.27906385
Delta E	71.1177	20.68039848
OTSU	170	49.23994639

The baseline ROI pixel area mean calculated from the original image was 100.3642. Since this is the baseline, standard deviation is zero. The mean ROI pixel area value for HSV was 81.5484, the corresponding values for K-Means, Delta E and OTSU were 74.5137, 71.1171 and 170 respectively.

The standard deviation values denote the degree of deviance from baseline. HSV has the least deviance, followed by KMeans. OTSU has the highest variance from baseline in this study. The following chart shows the accuracy of computed ROI's by different algorithms.



The confusion matrix was tabulated based on the sample size of 17 images that were used to calculate the various statistical measures that are a part of this study. The hypothesis that was

postulated was an accurate extraction of the intended regions of interest in all 17 images that were used to test the algorithms.

Predicted YES :	17
(All ROIs will be completely Extracted)	
Predicted NO :	0
(All ROIs will NOT be completely Extracted)	

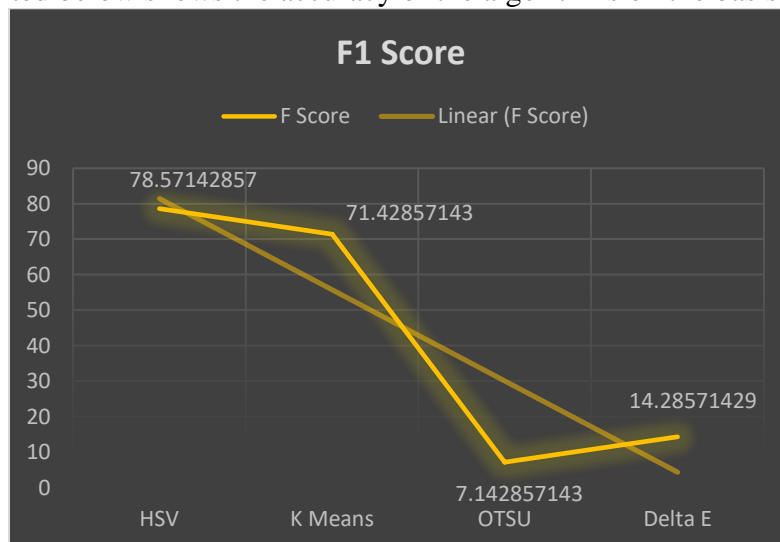
The various metrics that were calculated can be found below:

	Accuracy	Misclassification Rate	True Positive Rate	Precision	F-Score
HSV	70.58824	29.41176471	100	64.70588	78.57143
K-Means	64.70588	35.29411765	90.90909091	58.82353	71.42857
OTSU	29.41176	70.58823529	9.090909091	5.882353	7.142857
Delta E	23.52941	76.47058824	18.18181818	11.76471	14.28571

The accuracy of the various algorithms in extracting the ROI's can be found above. HSV had the maximum accuracy in extraction and Delta E scored the least in this particular measure. To extrapolate the results further, the F1 scores of all these algorithms were calculated. The F1 score is a measure of algorithmic mean accuracy and is calculated using the formula:

$$F1 = 2 * (Precision * Recall)/(Precision + Recall)$$

The graph presented below shows the accuracy of the algorithms on the basis of their F1 scores.



As can be seen, the results are placed in the decreasing order of F1 accuracy with HSV scoring the maximum and OTSU scoring the least.

## 5. Findings

It was found that HSV was most effective in extracting the target Regions of interest and the OTSU algorithm presented the least capacity to extract the target regions of interest from the image set.

## 6. Conclusions & Recommendations

In general, fMRI segmentation is not a trivial task, because acquired MR images are imperfect and are often corrupted by noise and other image artifacts. (Sharma et al 2010) point out that fMRI images have the following elements that can create problems during segmentation. They state that a fMRI image will have a) Partial Volume b) RF Noise c) Intensity in homogeneity d) Gradient e) Wrap Around f) Motion. Algorithms therefore have to be properly preprocessed and careful analysis of an image segmentation algorithm is therefore necessary. Due to the rapid development of medical image modalities, new application-specific segmentation problems are emerging and new methods are continuously explored and introduced.

Selection of the most appropriate technique for a given application is a difficult task. In many cases, a combination of several techniques may be necessary to obtain the segmentation goal. Very often integration of multimodal can help to segment structures that otherwise could not be detected on single images.

## 7. Future Work

The importance of image segmentation in medicine and medical analysis is clearly underscored. In the future, image segmentation algorithms will have to work in real time, with larger volumes of data and this implies that the efficiency and speed with which these algorithms operate in extracting ROI's would need to be higher. The future course of action with respect to this study would be to: a) develop new methods of analyzing image segmentation efficiency so that they are better suited for real time analysis. b) develop efficient variants of the algorithms that were studied and fine tune their accuracy of ROI extraction.

## Acknowledgements

All images that were used in this paper were kindly provided with express consent by M/s Mahajan Imaging Ltd, New Delhi. The scans were all masked properly to maintain patient confidentiality.

I would like to acknowledge the efforts of the teaching staff members of department of M.Sc. CST, women's Christian college for providing the impetus to successfully complete this study.

## References

- [1] Racine et al, (2005) - Nat Rev Neurosci. 2005 Feb; 6(2): 159–164.
- [2] Knutson et al, (2004) - Inferring Affect From Fmri Data, Department Of Psychology, Stanford University, Stanford, CA 94305, USA. TICS-1330;
- [3] Vrij et al, (2000) - Detecting Deceit Via Analysis Of Verbal And Nonverbal Behavior, Journal Of Nonverbal Behavior 24(4)
- [4] Saxe (2016), Lying: Thoughts Of An Applied Social Psychologist, American Psychologist 46 (4), 409.
- [5] Depaulo(2004), Serious Lies, Basic And Applied Social Psychology,26(2&3), 147–167.
- [6] Kesavadas et al (2007), Real-Time Functional MR Imaging (Fmri) For Presurgical Evaluation Of Paediatric Epilepsy, Pediatric Radiology 37.10 (2007): 964-974.
- [7] Boynton et al, 1996; - Linear Systems Analysis Of Functional Magnetic Resonance Imaging In Human V1, Neuroimage 16(13), January 1998
- [8] Buckner et al, 1996, Event-Related fMRI and the Hemodynamic Response, Human brain mapping 6.
- [9] Cabeza et al, 2007 - Trusting Our Memories: Dissociating the Neural Correlates of Confidence in Veridical vs. Illusory Memories. J Neurosci. 2007; 27:12190–12197.
- [10] Suzuki et al, 2008 - Neural Correlates Of True Memory, False Memory, And Deception.Cereb Cortex. 2008 Dec; 18(12): 2811–2819.
- [11] Smith et al, 2004 - Probabilistic Independent Component Analysis For Functional Magnetic Resonance Imaging.IEEE Trans Med Imag,23(2):137–152.
- [12] Smith et al, 2004 - Advances in Functional and Structural MR Image Analysis and Implementation as FSL, Oxford University.
- [13] Despotovic et al, 2015 - MRI Segmentation Of The Human Brain: Challenges, Methods, And Applications, Computational And Mathematical Methods In Medicine Volume 2015.
- [14] Nourouzi et al 2014 - Medical Image Segmentation Methods, Algorithms, And Applications,IETE Technical Review 31(3):199-213,June 2014.
- [15] Wee et al, 2006 - Current Methods in the Automatic Tissue Segmentation of 3D Magnetic Resonance Brain Images, Current Medical Imaging Reviews, 2006, 2, 000-000.
- [16] Kumar et al, 2016 - Image Processing In Diabetic Related Causes, Forensic and Medical Bioinformatics
- [17] Bora et al, 2015 - Clustering Approach Towards Image Segmentation: An Analytical Study, International Journal Of Research In Computer Applications And Robotics, Vol.2 Issue.7, Pg.: 115-124
- [18] Sharma et al 2010, The Relationship Between Motor Deficit And Primary Motor Cortex Hemispheric Activation Balance After Stroke: Longitudinal Fmri Study. Journal Of Neurology, Neurosurgery & Psychiatry.

---

\*Corresponding author.

E-mail address: arthiciyer@gmail.com